
Finetuning Pretrained Vision-Language Models with Correlation Information Bottleneck for Robust Visual Question Answering

Jingjing Jiang, Ziyi Liu, Nanning Zheng

Institute of Artificial Intelligence and Robotics, Xi'an Jiaotong University

jingjingjiang2017@gmail.com, {liuziyi@stu, nnzheng@mail}.xjtu.edu.cn

Abstract

Benefiting from large-scale Pretrained Vision-Language Models (VL-PMs), the performance of Visual Question Answering (VQA) has started to approach human oracle performance. However, finetuning large-scale VL-PMs with limited data for VQA usually faces overfitting and poor generalization issues, leading to a lack of robustness. In this paper, we aim to improve the robustness of VQA systems (*i.e.*, the ability of the systems to defend against input variations and human-adversarial attacks) from the perspective of Information Bottleneck when finetuning VL-PMs for VQA. Generally, internal representations obtained by VL-PMs inevitably contain irrelevant and redundant information for the downstream VQA task, resulting in statistically spurious correlations and insensitivity to input variations. To encourage representations to converge to a minimal sufficient statistic in vision-language learning, we propose the Correlation Information Bottleneck (CIB) principle, which seeks a tradeoff between representation compression and redundancy by minimizing the mutual information (MI) between the inputs and internal representations while maximizing the MI between the outputs and the representations. Meanwhile, CIB measures the internal correlations among visual and linguistic inputs and representations by a symmetrized joint MI estimation. Extensive experiments on five VQA benchmarks of input robustness and two VQA benchmarks of human-adversarial robustness demonstrate the effectiveness and superiority of the proposed CIB in improving the robustness of VQA systems.

1 Introduction

Visual Question Answering (VQA) [1] is a classical vision-language task. Recently, the large-scale Pretrained Vision-Language Models (VL-PMs) [2–4] have elevated the VQA performance to the level of human oracle. However, finetuning extremely large-scale VL-PMs with limited data for the downstream VQA task usually suffers from overfitting and poor generalization issues, making the improvement in VQA robustness brought by VL-PMs relatively limited and far less than the improvement in VQA accuracy.

In this paper, we explore two types of VQA robustness, namely, input robustness and human-adversarial robustness, and aim to improve the robustness when finetuning VL-PMs for VQA. The input robustness refers to the capability of VQA models to defend against visual variations in images (*e.g.*, question-related object removal [5]) and linguistic variations in questions (*e.g.*, word substitution and sentence rephrasing [6, 7]). The human-adversarial robustness is the ability of VQA models to defend against adversarial attacks by human [8, 9]. Practically, in the finetuning process, VQA is usually formulated as a multi-answer classification problem where VL-PMs act as representation extractors with rich knowledge, and the extracted vision-language representation are passed to

an additional VQA Head module for answer prediction. As such, improving the two robustness essentially makes the obtained representation more compact and task-related.

To this end, we propose to improve the robustness from an Information-theoretical perspective. From this view, one possible reason for poor VQA robustness is that representations yielded by VL-PMs inevitably contain irrelevant and redundant information for the downstream VQA task. Specifically, the irrelevant information will encourage VQA systems to learn statistically spurious correlations between representations and labels, while task-agnostic redundant information will reduce the sensibility of VQA systems to input variations. Both types of information will impair the VQA robustness. Therefore, to obtain more robust representations when finetuning VL-PMs for VQA, we expect to discard irrelevant and redundant information in representations while preserving the relevant information. The Information Bottleneck (IB) principle [10] can seek a tradeoff between representation compression and redundancy. Motivated by this, we exploit the IB principle to find the minimal sufficient statistic of the obtained representations for more robust VQA systems.

We propose Correlation Information Bottleneck (CIB) to improve the robustness of VQA systems when finetuning VL-PMs for VQA. Specifically, CIB promotes the vision-language representations to converge to a minimal sufficient statistic by minimizing mutual information (MI) between the representations and inputs while maximizing MI between the representations and outputs. In addition to the overall dependency between inputs and the vision-language representations, we utilize a symmetrized joint MI to measure the internal correlations among visual and linguistic representations and inputs, guiding VQA systems to better capture the actual correlations. Furthermore, to consider different architectures of VL-PMs (*i.e.*, the single-stream and two-stream Transformer layers), we unify the internal representations of different VL-PMs for CIB estimation.

To demonstrate the proposed CIB principle, we first provide a rigorous theoretical derivation of the lower bound of CIB. Then, we apply it to finetune five baseline VL-PMs on five VQA benchmarks of input robustness and two VQA benchmarks of human-adversarial robustness. Extensive experiments consistently show that CIB can significantly improve the robustness of VQA systems and show the superiority of CIB compared with existing methods.

2 Method

In this section, we first state the preliminary of VQA and the general IB principle, then introduce the proposed Correlation Information Bottleneck (CIB) and explain how CIB is applied to finetune Pretrained Vision-Language Models (VL-PMs) for VQA.

2.1 Preliminary

Problem Setting. In the finetuning process, the VQA task is formulated as a multi-answer classification problem. Given a VQA dataset $\mathcal{D} = \{(I, Q, y) \in \mathcal{I} \times \mathcal{Q} \times \mathcal{Y}\}$, where I is an image, Q is a question, and y is an answer, VL-PMs take image-question pairs as input, where the image is further represented as a set of image regions $\{v_1, \dots, v_K\}$ (K is the number of regions in one image) and the question is tokenized as a token sequence $\{w_1, \dots, w_L\}$ (L is the number of word tokens in a question), and output the answer probability distribution Y using a additional VQA Head module (*i.e.*, two fully-connected layers sandwiched with GeLU activation and Layer Normalization operation).

IB View of Representation Learning. From an information-theoretical view, seeking a robust representation T for VL-PMs is equivalent to preserving information about the output Y while removing irrelevant and redundant information from the input X . This is because for the given VQA task, the irrelevant and redundant information may encourage VL-PMs to learn superfluous correlations between answer labels and inputs. Formally, the IB principle [10, 11] formulates vision-language representation learning as an information-theoretic tradeoff and finds an optimal representation by maximizing the Lagrangian

$$\mathcal{L}_{\text{IB}} := I(Y; T) - \beta I(X; T), \quad (1)$$

where $\beta \geq 0$ controls the tradeoff between compression and prediction, and $I(\cdot; \cdot)$ denotes mutual information (MI).

2.2 Correlation Information Bottleneck

In vision-language representation learning, given the two modal inputs X^v and X^l , T^v and T^l denote the corresponding internal visual and linguistic representations. To extend the general IB principle to this setting, we group the input sources and internal representations as $X = [X^v, X^l]$ and $T = [T^v, T^l]$. Therefore, the training objective is to learn the minimal sufficient representation T that discards all irrelevant and redundant information from the input X for the given VQA task.

Specifically, to derive a differentiable IB estimation in vision-language representation learning, we first focus on the term $I(Y; T)$ in Eq.(1), which can be rewritten as the following form using conditional probability definition:

$$I(Y; T) = \int p(y, t) \log \frac{p(y|t)}{p(y)} dy dt. \quad (2)$$

Since the conditional probability $p(y|t)$ is intractable, we instead estimate $I(Y; T)$ with the BA [12] lower bound:

$$I(Y; T) \geq \int p(y, t) \log q(y|t) dy dt - \int p(y) \log p(y) dy, \quad (3)$$

where $q(y|t)$ is an accessible auxiliary distribution of $p(y|t)$, and the entropy of labels $H(Y) = - \int p(y) \log p(y) dy$ is independent for the optimization procedure. Ignoring $H(Y)$, the remaining term in Eq.(3) is equal to $-H(Y|T)$, meaning that maximizing the lower bound of $I(Y; T)$ is equivalent to minimizing the cross-entropy loss of the given task.

Next, we consider the mutual information between the input sources and their corresponding representations, *i.e.*, $I(X; T)$ in Eq.(1). In addition to measuring the overall dependency between X and T (*i.e.*, regarding visual and linguistic representations as one), we also concerns the internal correlations among X^v , X^l , T^v , and T^l , which can guide VL-PMs to learn correlations between visual and linguistic representations. Therefore, we propose to maximize the Correlation Information Bottleneck (CIB) formula:

$$\mathcal{L}_{\text{CIB}} := I(Y; T) - \beta I(X^v, X^l; T^v, T^l), \quad (4)$$

where, $I(X^v, X^l; T^v, T^l)$ can be regarded as a symmetrized variant of joint mutual information [13] that considers the relevance of the input set and the relevance of the representation set. To efficiently approximate $I(X^v, X^l; T^v, T^l)$, we first expand it conditioned on the properties of mutual information and the data processing inequality in representation learning [14]. The derivation can be formally stated by Theorem 1 (see Appendix for proof):

Theorem 1. (*Upper Bound of $I(X^v, X^l; T^v, T^l)$*) Given two groups of random variables $X = [X^v, X^l]$, $T = [T^v, T^l]$, the mutual information $I(X^v, X^l; T^v, T^l)$ can be upper-bounded with

$$I(X; T) = I(X^v, X^l; T^v, T^l) \leq \underbrace{I(X^v; T^v)}_{\textcircled{1}} + \underbrace{I(X^l; T^l)}_{\textcircled{2}} - \underbrace{I(T^v; T^l)}_{\textcircled{3}} + \underbrace{D_{\text{SKL}}}_{\textcircled{4}}, \quad (5)$$

where D_{SKL} denotes the Symmetric Kullback-Leibler divergence and can be obtained by averaging the two Kullback-Leibler divergence, $D_{\text{KL}}(p(t^v|x^v)||p(t^l|x^l))$ and $D_{\text{KL}}(p(t^l|x^l)||p(t^v|x^v))$.

Afterwards, we follow Wang *et al.* [15] to further upper-bound MI between the input and its representation with a localized formulation of IB. Formally, for the visual and linguistic inputs X^v , X^l , they are essentially two sets of random variables, *i.e.*, $X^v = [X_1^v, X_2^v, \dots, X_K^v]$, $X^l = [X_1^l, X_2^l, \dots, X_L^l]$, f_{θ^v} and f_{θ^l} are the two functions that map X^v and X^l into visual and linguistic representations, *i.e.*, $T^v = [T_1^v, T_2^v, \dots, T_K^v] = [f_{\theta^v}(X_1^v), f_{\theta^v}(X_2^v), \dots, f_{\theta^v}(X_K^v)]$ and $T^l = [T_1^l, T_2^l, \dots, T_L^l] = [f_{\theta^l}(X_1^l), f_{\theta^l}(X_2^l), \dots, f_{\theta^l}(X_L^l)]$. The MI between the visual/linguistic input and the visual/linguistic representation can be maximized by

$$I(X^v; T^v) \leq K \sum_{i=1}^K I(X_i^v; T_i^v); \quad I(X^l; T^l) \leq L \sum_{i=1}^L I(X_i^l; T_i^l). \quad (6)$$

Therefore, the lower bound of \mathcal{L}_{CIB} can be stated as Theorem 2.

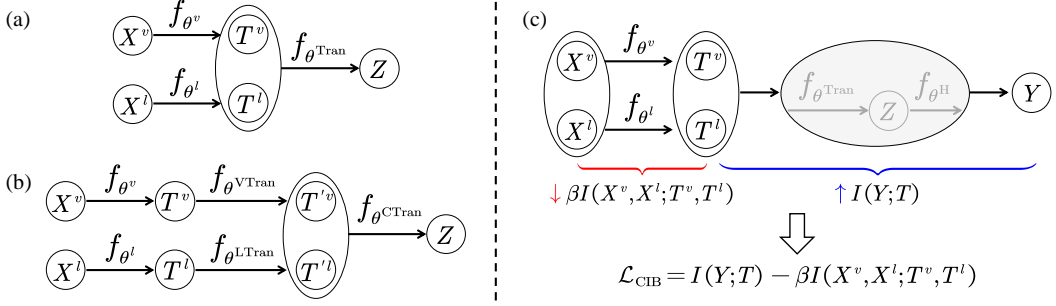


Figure 1: (a) The information flow of single-stream VL-PTMs. (b) The information flow of two-stream VL-PTMs. (c) The proposed CIB unifies the two typical VL-PTMs architectures. Seeking the minimal sufficient statistic by minimizing MI between inputs and the internal representations (↓) while maximizing MI between outputs and the representations (↑).

Theorem 2. (Lower Bound of \mathcal{L}_{CIB}) Given two groups of random variables, $X = [X^v, X^l]$ and $T = [T^v, T^l]$, where X^v , X^l , T^v , and T^l are represented as the sets of random variables, i.e., $X^v = [X_1^v, X_2^v, \dots, X_K^v]$, $X^l = [X_1^l, X_2^l, \dots, X_L^l]$, $T^v = [T_1^v, T_2^v, \dots, T_K^v]$, and $T^l = [T_1^l, T_2^l, \dots, T_L^l]$. Two deterministic functions, f_{θ^v} and f_{θ^l} , make $T^v = [T_1^v, T_2^v, \dots, T_K^v] = [f_{\theta^v}(X_1^v), f_{\theta^v}(X_2^v), \dots, f_{\theta^v}(X_K^v)]$, $T^l = [T_1^l, T_2^l, \dots, T_L^l] = [f_{\theta^l}(X_1^l), f_{\theta^l}(X_2^l), \dots, f_{\theta^l}(X_L^l)]$. Then, the formulation of Correlation Information Bottleneck (CIB) can be lower-bounded with

$$\begin{aligned} \mathcal{L}_{CIB} &= I(Y; T) - \beta I(X^v, X^l; T^v, T^l) \\ &\geq I(Y; T) - \beta \left[D_{\text{SKL}} - I(T^v; T^l) + K \sum_{i=1}^K I(X_i^v; T_i^v) + L \sum_{i=1}^L I(X_i^l; T_i^l) \right]. \end{aligned} \quad (7)$$

The theorem indicates that in vision-language representation learning, once $I(Y; T)$ is regarded as a task-related objective, $-\beta I(X^v, X^l; T^v, T^l)$ can be used to constrain the representation compactness so that to seek robust representations by the tradeoff between redundancy and compression.

2.3 Finetuning VL-PMs for VQA with Correlation Information Bottleneck

As shown in Figure 1 (a) and (b), there are two typical transformer architectures of VL-PMs: the single-stream [16–18] and the two-stream [19, 20]. When finetuning VL-PMs for VQA, to unify the two typical architectures into one formulation, as shown in Figure 1 (c), we utilize the region-level features after the visual Embedding layer (i.e., f_{θ^v} is the parametric Embedding layer) as the internal visual representation T^v . Analogously, the token-level features after the linguistic Embedding layer (f_{θ^l}) is regarded as the internal linguistic representation T^l . All the following Transformer layers ($f_{\theta^{\text{Tran}}}$) and the VQA Head module ($f_{\theta^{\text{H}}}$) serve as the parametric approximator to yield Y given $T = [T^v, T^l]$. In summary, to utilize CIB to finetune VL-PMs for VQA, we regard $I(Y; T)$ in Eq.(7) as the task-related loss (i.e., the cross-entropy loss for answer prediction), and the remaining terms in Eq.(7) can be considered as regularizers.

Estimating MI Terms in \mathcal{L}_{CIB} . In the finetuning process, for sample pairs $\{(X_i^v, T_i^v)\}_{i=1}^K$ and $\{(X_i^l, T_i^l)\}_{i=1}^L$, the conditional probability distributions $p(t^v|x^v)$ and $p(t^l|x^l)$ are known. We thus adopt a sample-based differentiable MI estimator, CLUB [21], to approximate the upper bound of MI between the visual/linguistic inputs and the corresponding representations, i.e.,

$$\hat{I}(X^v; T^v) = \frac{1}{K^2} \sum_{i=1}^K \sum_{j=1}^K \left[\log p(t_i^v|x_i^v) - \log p(t_j^v|x_i^v) \right], \quad (8)$$

$$\hat{I}(X^l; T^l) = \frac{1}{L^2} \sum_{i=1}^L \sum_{j=1}^L \left[\log p(t_i^l|x_i^l) - \log p(t_j^l|x_i^l) \right]. \quad (9)$$

For $I(T^v; T^l)$, it is difficult to be estimated directly due to the different sequence lengths of $T^v \in \mathbb{R}^{K \times d}$ and $T^l \in \mathbb{R}^{L \times d}$. Thus, we first transform the sequence representations into global visual

Table 1: Quantitative results on input robustness and human-adversarial robustness. More complete comparisons with existing methods on corresponding benchmarks are available at Appendix.

	Models	Input Robustness					Adversarial Robustness				
		VQA-Rep		VQA P2		IV-VQA	CV-VQA	VQA-CE	AVQA	AdVQA	
Pert CS(4)		Pert CS(2)		Pert	Pert	CE	test	val	test	val	
Training on		VQA v2 train split							AVQA train split		
	SoTA	56.59	58.95	68.10	74.40	-	-	39.24	26.08	27.08	
ID	VisualBERT	62.03	55.06	68.23	72.34	46.04	30.48	38.75	23.84	24.01	
	+ CIB	63.10	56.31	69.92	73.83	47.81	32.46	40.86	24.55	24.78	
	Δ	+1.07	+1.25	+1.69	+1.49	+1.77	+1.98	+2.11	+0.71	+0.77	
ID + OOD	UNITER _B	62.68	55.66	70.36	74.36	75.71	42.60	40.64	24.50	25.49	
	+ CIB	64.45	58.75	71.30	75.91	76.63	46.92	42.03	25.71	25.89	
	Δ	+1.77	+3.09	+0.94	+1.55	+0.92	+4.32	+1.39	+1.21	+0.40	
	LXMERT	70.41	65.21	77.30	82.96	77.83	40.16	53.61	25.17	25.77	
	+ CIB	72.62	67.71	78.93	85.07	78.57	40.47	57.14	26.18	26.15	
	Δ	+2.21	+2.50	+1.63	+2.11	+0.74	+0.31	+3.53	+1.01	+0.38	
OOD	ViLBERT	59.16	51.22	67.18	71.39	72.37	32.24	36.94	25.27	25.83	
	+ CIB	62.28	55.89	69.92	73.98	74.09	34.10	39.51	26.55	26.49	
	Δ	+3.12	+4.67	+2.74	+2.59	+1.72	+1.86	+2.57	+1.28	+0.66	
	VL-BERT _B	59.89	52.99	68.36	72.52	72.42	33.52	36.56	25.25	25.47	
	+ CIB	60.86	53.89	69.82	73.88	73.66	35.29	38.24	26.35	26.38	
	Δ	+0.97	+0.90	+1.46	+1.36	+1.24	+1.77	+1.68	+1.10	+0.91	
Avg.		+1.83	+2.48	+1.69	+1.82	+1.28	+2.05	+2.26	+1.06	+0.63	
										+1.10 +1.18	

and linguistic representations, $\bar{T}^v \in \mathbb{R}^d$ and $\bar{T}^l \in \mathbb{R}^d$, using two one-layer fully-connected (FC) networks. Then, to guarantee the inequality in Eq.(7) hold, we should approximate the lower bound of $I(T^v; T^l)$. Therefore, we lower-bound it with NWJ [22], *i.e.*,

$$\hat{I}(\bar{T}^v; \bar{T}^l) = \mathbb{E}_{p(\bar{T}^v, \bar{T}^l)} [\log f(\bar{T}^v, \bar{T}^l)] - \frac{1}{e} \mathbb{E}_{p(\bar{T}^v)p(\bar{T}^l)} [f(\bar{T}^v, \bar{T}^l)], \quad (10)$$

where f is a discriminant function implemented by a two-layer FC network.

Estimating D_{SKL} in \mathcal{L}_{CIB} . Since $p(t^l|x^l)$ and $p(t^v|x^v)$ have a known probability density, we directly compute the symmetric Kullback-Leibler divergence D_{SKL} .

3 Experiments

The goal of our experiments is to verify whether using CIB as a training objective when finetuning VL-PMs for VQA will make VQA systems more robust. Specifically, we consider the following questions: (1) Facilitated by CIB, does the VL-PMs learn more robust representations than vanilla VL-PMs? (2) How does each component of CIB contribute to the VQA robustness?

Shared Implementation Details. In all following experiments, the image region features are extracted using bottom-up attention Faster R-CNN [23] pre-trained on Visual Genome [24]. For all baseline VL-PMs, the number of word tokens L is set as 20. The number of image regions K for LXMERT and VisualBERT are 36 and 100, respectively. For UNITER_B, ViLBERT, and VL-BERT_B, K is not fixed. The dimension d of representation is 768. All experiments are implemented using PyTorch on one NVIDIA GTX2080 12GB GPU. As for optimization, we utilize AdamW optimizer with a linear warmup with linear decay, a warmup step of 1000, a batch size of 64, and a peak learning rate of 2e-5. The total number of training epochs is 10.

3.1 Evaluation on Input Robustness

Experimental Settings. In this experiments, we utilize five typical VL-PMs as baselines (*i.e.*, VisualBERT [16], UNITER_B [18], LXMERT [19], VL-BERT_B [17], and ViLBERT [20]) and evaluate our CIB objective on five VQA benchmarks of input robustness (*i.e.*, VQA-Rep [6], VQA P2 [7], IV-VQA [5], CV-VQA [5], and VQA-CE [25]). Specifically, VQA-Rep and VQA P2 evaluate the robustness against linguistic variations, IV-VQA and CV-VQA evaluate robustness w.r.t. visual variations, and VQA-CE evaluates the robustness against shortcut learning involving inputs. *Note that all these benchmarks of input robustness are built on VQA v2 val split, we thus only finetune*

our models on VQA v2 training set. In addition, since the images of VQA v2 are derived from COCO [26], we follow the works [18] to divide these VL-PMs into ID (in-domain), ID+OOD (in-domain + out-domain), and OOD (out-domain) according to whether they use the COCO dataset in the pretraining process. The more detailed statistics of the benchmarks are shown in Appendix.

Metrics. In addition to the standard evaluation metric, *i.e.*, the VQA-Score, we follow Shah *et al.* [6] to evaluate the robustness against linguistic variations using Consensus Score (CS(k)). Specifically, CS(k) is the ratio of the number of subsets where all questions are answered correctly to the total number of subsets of size k . For each question group Q with one original question and corresponding n rephrasings, all subsets with size k are nC_k , then CS(k) is defined as

$$\text{CS}(k) = \sum_{Q' \subset Q, |Q'|=k, q \in Q'} \frac{\mathbb{1}_{\Theta}(q)}{{}^nC_k}, \quad (11)$$

where, Θ is a set where the answer of question q is correct, and $\mathbb{1}$ is an indicator function defined on Θ . Obviously, *the higher the average consensus score at higher values of k , the more robust the model is*. Since the baseline VL-PMs partly use the original examples of robustness benchmarks, which would result in unreliable VQA-Score on original examples, we only test the VQA-Score of perturbed examples (Pert) and counterexamples (CE).

Experimental Results. The results are shown in Table 1. We see that compared with baselines (*i.e.*, finetuning VL-PMs for VQA with only the cross-entropy loss for answer prediction), using CIB as the additional training objective can significantly improve the input robustness of VQA systems. In general, the results on the five VQA benchmarks of input robustness consistently show that it is feasible to encourage VL-PMs to learn more compact and robust representations from an information-theoretic perspective. In addition, from the comparisons between different baseline VL-PMs, we see that the CIB objective is effective for different architectures and domains.

3.2 Evaluation on Human-Adversarial Robustness

Experimental Settings. In this part, we also consider the above mentioned five baseline VL-PMs and stress test the VQA models finetuned with the CIB objective on two VQA benchmarks of human-adversarial robustness (*i.e.*, AVQA [8] and AdVQA [9]). Specifically, AVQA is built on images from out-of-domains (excluding COCO images), with $\sim 142.1\text{K}/8.7\text{K}/26.4\text{K}$ image-question pairs in the train/val/test split. AdVQA is based on VQA v2 images from COCO, with $\sim 10\text{K}/36.8\text{K}$ image-question pairs for val/test split. We uniformly finetune all models on AVQA train split and evaluate them on val and test splits of the two benchmarks.

Experimental Results. The results are shown in Table 1. Overall, the results on AVQA and AdVQA consistently illustrate the effectiveness of CIB for improving the human-adversarial robustness of VQA systems, demonstrating that using CIB as the training objective can facilitate VL-PMs to learn more adversarially robust representations. In addition, we observe that the performance improvement of CIB for human-adversarial robustness is not significant as the performance improvement for input robustness. One possible reason is that compared to the VQA benchmarks of input robustness, there is less irrelevant and redundant information between the question token-wise representations of human-adversarial VQA benchmarks.

3.3 Evaluation on Standard VQA Benchmark

To analyze the impact of CIB on the standard VQA performance (*i.e.*, whether the compression of internal representations of VL-PMs impairs the general VQA performance), we utilize CIB as the objective to train the aforementioned baseline VL-PMs on the VQA v2 training and validation sets. The results on VQA v2 test-dev are shown in Table 2 (Since we do not use the additional question-answer pairs from Visual Genome like UNITER_B [18] for data augmentation in our experiments and some other detail differences, there are minor differences between our re-implementation of baseline VL-PMs and the original paper results). Overall, training baseline VL-PMs with the proposed CIB can slightly improve

Table 2: Results on VQA v2 test-dev set. \dagger denotes our re-implementations of baseline VL-PMs.

Models	VQA-Score (%)	
	Baseline	+ CIB
VisualBERT[16]	70.80 (70.46 \dagger)	71.62 (+1.16)
UNITER _B [18]	72.70 (71.63 \dagger)	72.11 (+0.48)
LXMERT[19]	72.42 (72.58 \dagger)	72.99 (+0.41)
ViLBERT[20]	70.55 (70.55 \dagger)	71.00 (+0.45)
VL-BERT _B [17]	71.16 (71.20 \dagger)	71.59 (+0.39)

the standard VQA performance. We thus find that a certain degree of compression of representations can make the obtained representations more compact and robust, and facilitate VL-PMs to learn more true correlation between representations and labels.

3.4 Ablation Study

In this section, we utilize UNITER_B [18] and LXMERT [19] as representatives of the baseline VL-PMs, and conduct all ablated experiments on VQA-Rep [6] and AVQA [8].

Impact of CIB terms.

To analyze how different components of CIB contribute to the VQA robustness, we perform ablation study on different meaningful combinations of the terms in Eq.(5). Specifically, there are three other meaningful combinations: ▶ $\frac{3}{2} [I(X^v; T^v) + I(X^l; T^l)]$ (i.e., ① + ②), ▶ $-I(T^v; T^l) + D_{SKL}$ (i.e., ③ + ④), and ▶ $I(X^v; T^v) + I(X^l; T^l) + D_{SKL}$ (i.e., ① + ② + ④). The

results in Table 3 for different combinations of CIB terms are consistent in general, empirically demonstrating that the proposed CIB formula is a more tight upper bound of $I(X^v, X^l; T^v, T^l)$.

Table 3: Ablation study on the impact of different terms in CIB.

	CIB				VQA-Rep					AVQA val
	①	②	③	④	Pert	CS(1)	CS(2)	CS(3)	CS(4)	
UNITER _B	✓	✓			62.68	71.45	63.72	59.01	55.66	25.49
			✓	✓	64.07	72.73	65.51	61.03	57.82	25.27
	✓	✓	✓		64.11	72.82	65.61	61.18	57.99	25.55
	✓	✓	✓	✓	63.23	71.94	64.40	59.85	56.62	24.78
LXMERT	✓	✓	✓	✓	64.45	73.18	66.21	61.88	58.75	25.89
					70.41	79.73	72.93	68.49	65.21	25.77
	✓	✓			72.17	81.61	74.99	70.63	67.34	26.00
			✓	✓	72.07	81.56	74.77	70.26	66.87	26.07
	✓	✓	✓		72.28	81.70	74.94	70.43	67.06	25.89
	✓	✓	✓	✓	72.62	82.01	75.46	71.05	67.71	26.15

results in Table 3 for different combinations of CIB terms are consistent in general, empirically demonstrating that the proposed CIB formula is a more tight upper bound of $I(X^v, X^l; T^v, T^l)$.

Impact of MI Estimator.

Practically, any sample-based upper bound estimator of MI can be utilized to approximate $I(X^v; T^v)$ and $I(X^l; T^l)$, and any differentiable MI lower bound estimator can be applied to approach to $I(T^v; T^l)$. To analyze the impact of different MI estimators on CIB, we consider the following settings: (i) alternately using L1Out [22] instead of CLUB [21] as the MI upper bound estimator to approximate $I(X^v; T^v)$ and $I(X^l; T^l)$. (ii) approximating $I(T^v; T^l)$ with the other three MI lower bound estimators, InfoNCE [28], NWJ [27], and MINE [29]. Table 4 shows the VQA-Score of perturbed examples on VQA-Rep and the results on AVQA val of different MI estimators, which consistently demonstrates that the effectiveness of CIB in improving the input robustness of VQA systems does not depend on a specific MI estimator.

Impact of different internal representations of two-stream VL-PMs.

For the two-stream VL-PMs, as shown in Figure 1 (b), there is an alternative form of the obtained internal representations $T = [T^v, T^l]$, i.e., the visual and linguistic representations after the Vision-Transformer layers ($f_{\theta VTran}$) and Language-Transformer layers ($f_{\theta LTran}$). When finetuning two-stream VL-PMs with CIB for VQA, to analyze the impact of different internal representations, we replace the original $T = [T^v, T^l]$ in \mathcal{L}_{CIB} with $T = [T'^v, T'^l]$. The results shown in Table 5 indicate that for two-stream VL-PMs, using the visual/linguistic representations after Vision/Language Transformer layers as the internal representations to estimate \mathcal{L}_{CIB} is also feasible.

Table 4: Ablation study on the impact of different MI estimators.

Models	MI Estimator		VQA-Score	
	Upper Bound	Lowe Bound	VQA-Rep	AVQA
UNITER _B			62.68	25.49
	L1Out [22]	NWJ [27]	64.27	25.54
	CLUB [21]	InfoNCE [28]	64.14	25.85
	CLUB [21]	MINE [29]	64.32	25.53
LXMERT	CLUB [21]	NWJ [27]	64.45	25.89
			70.41	25.77
	L1Out [22]	NWJ [27]	72.31	26.03
	CLUB [21]	InfoNCE [28]	72.34	26.11
	CLUB [21]	MINE [29]	72.48	25.98
	CLUB [21]	NWJ [27]	72.62	26.15

Table 5: Ablation study on the impact of different internal representations obtained by the two-stream VL-PTMs.

Models	\mathcal{L}_{CIB}		VQA-Score	
	VQA-Rep	AVQA	VQA-Rep	AVQA
LXMERT			70.41	25.77
	$I(Y; T) - \beta I(X^v, X^l; T'^v, T'^l)$		72.53	26.14
	$I(Y; T) - \beta I(X^v, X^l; T^v, T^l)$		72.62	26.15

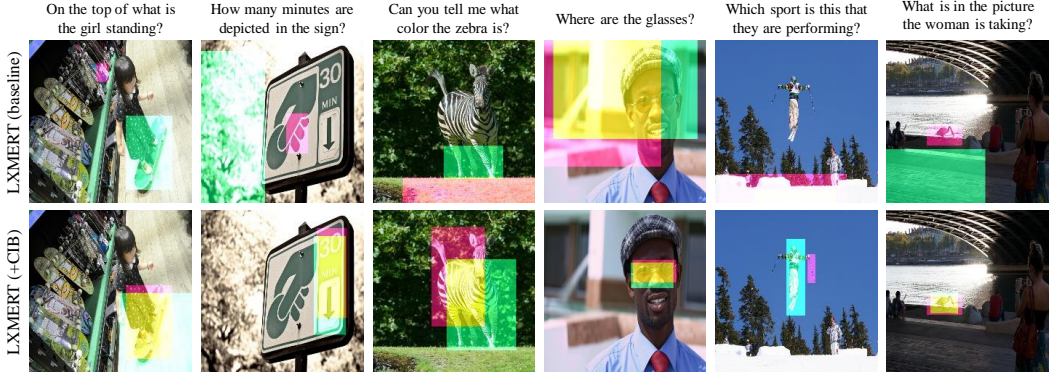


Figure 2: Visualization of the top two objects with the highest attention scores. The image-question pairs originate from VQA-Rep. Objects with the best and second attention scores are marked in magenta and green, respectively.

Sensibility of tradeoff β . β controls the tradeoff between representation redundancy and compression, which is the key hyperparameter of CIB. We thus perform a grid search for β . Specifically, we consider the following values: $\beta \in [1 \times 10^{-6}, 1 \times 10^{-5}, 5 \times 10^{-5}, 1 \times 10^{-4}, 5 \times 10^{-4}, 1 \times 10^{-3}, 5 \times 10^{-3}, 1 \times 10^{-2}, 5 \times 10^{-2}]$. Figure 3 shows the variation curve of the VQA-Score (Pert) on VQA-Rep and AVQA with increasing $\log \beta$. We observe that both on VQA-Rep and AVQA, the VQA-Scores start to boost when β is a quite small value, which indicates the effectiveness of CIB. When β increases to 5×10^{-5} and 1×10^{-4} , UNITER_B and LXMERT achieve the best performance, respectively. After that, the performance usually starts to drop, meaning that extremely compressed representations of VL-PMs may begin to compromise the robustness of VQA systems.

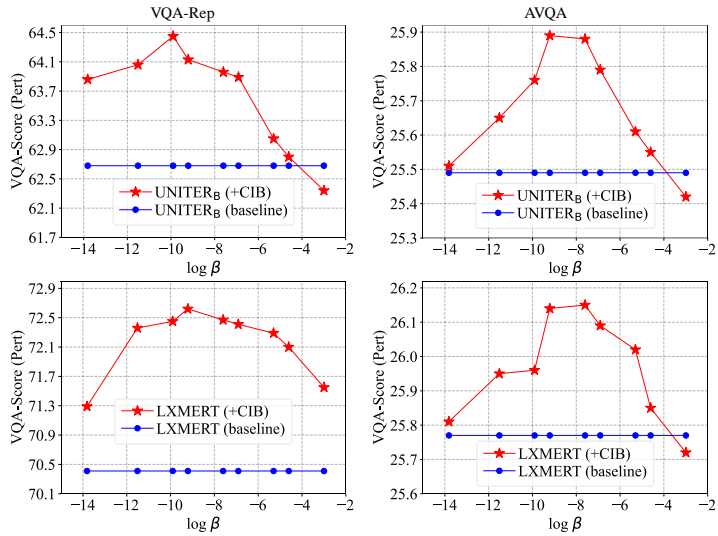


Figure 3: The variation curve of the VQA-Score (Pert) on VQA-Rep and AVQA as $\log \beta$ increases.

3.5 Qualitative Visualization

Why can CIB improve the VQA robustness when finetuning VL-PMs for VQA? To explore the possible reason, we first enumerate the image-question pairs of VQA-Rep whose answers are correctly predicted by LXMERT finetuned with CIB but incorrectly predicted by the baseline LXMERT (*i.e.*, finetuned without CIB). Then, we compute the attention score between the final representation $Z \in \mathbb{R}^d$ for answer prediction and the input visual representation $X^v \in \mathbb{R}^{K \times d}$ of object regions by $\text{score}_{\text{attn}} = \text{softmax}(Z \cdot (X^v)^T / \sqrt{d})$. Finally, we plot the top two objects with the highest attention scores in the image. From the results shown in Figure 2, we observe that compared with the baseline LXMERT, the attended two objects obtained by LXMERT finetuned with CIB are more consistent and question-related. This observation qualitatively illustrates that using CIB as an additional training objective to finetune VL-PMs for VQA can encourage the VQA systems to learn more discriminative representations for different answers and reduce the irrelevant information to questions.

4 Related Work

Robustness in VQA. Recently, in order to promote the practical application of VQA systems, many works have been proposed to study various VQA robustness, such as human-adversarial robustness [8, 9], input robustness [6, 7, 5, 30], and the robustness against answer distribution shift [31–35]. In this paper, we explore input robustness and human-adversarial robustness. The input robustness means the capability of VQA systems to defend against the visual and linguistic variations, such as rephrasing questions [6, 7], manipulating images [5]. The prevailing method to improve input robustness is data augmentation, generating additional data to train more robust VQA models. Besides, contrastive learning [30] and adversarial training [36] are also introduced to improve input robustness. While data augmentation is a feasible and effective solution, the quality of the generated data is uncontrollable (*e.g.*, limited expressiveness and excessive verbosity), and the human-generated process is time-consuming. The human-adversarial robustness is the capability of VQA systems to defend against adversarial attacks by human. More specifically, Li *et al.* [8] and Sheng *et al.* [9] consider adversarial attacks by human annotators on state-of-the-art VQA models and introduce two adversarial VQA benchmarks, AVQA and AdVQA, which consist of adversarial samples that can be answered correctly by human but not by state-of-the-art models. All recent studies demonstrate state-of-the-art VQA models are still vulnerable to input variations and adversarial attacks. In this paper, we propose to improve the robustness of VQA systems from an information-theoretic perspective.

Information Bottleneck (IB). The IB principle is originally proposed by Tishby *et al.* [10] for information compression, and is later applied to analyze deep learning model architectures [11, 37]. Essentially, the IB objective is to seek a tradeoff between maximizing the predictive accuracy and minimizing the representation complexity. Some recent researches target exploiting the IB principle to improve the model robustness and generalization, especially in Domain Generalization [38, 39], OOD Generalization [40], Multiview Representation Learning [14, 41], and finetuning of Pretrained Language Models [42, 15]. Besides, some works [43–45] aim to learn the disentangled optimal representation from an IB perspective. Since IB can facilitate compact and meaningful representations learning, we extend it to vision-language learning and apply it to obtain robust VQA systems.

Pretrained Vision-Language Models (VL-PMs). Vision-Language pretraining aims to learn task-agnostic visiolinguistic representations for improving the performance of downstream tasks in a finetuning fashion [46–52]. From the perspective of model architecture, prevailing VL-PMs models can be roughly grouped into two types: single-stream models [17, 18, 53–55, 50] and two-stream models [20, 19, 56–58]. Specifically, the single-stream models first align image regions and text words and then apply a uniform transformer [59] to learn the contextualized representations. The two-stream models first use two separate transformers to learn high-level representations of image and text, and then integrate the two modalities with a cross-modal transformer. In this paper, we unify the two typical types of VL-PMs models and propose CIB to improve the VQA robustness when finetuning the two types of VL-PMs for VQA.

5 Conclusion and Discussion

Conclusion. In this paper, we propose to improve the robustness of VQA systems when finetuning VL-PMs for VQA from the Information Bottleneck perspective. Specifically, we first derive a new IB lower bound (CIB) for vision-language learning, and then apply CIB to finetune VL-PMs for VQA. Extensive experiments on five VQA benchmarks of input robustness and two VQA benchmarks of human-adversarial robustness consistently demonstrate the effectiveness and superiority of CIB. In the future, we plan to assess the effectiveness of CIB when tuning VL-PMs for VQA using parameter-effective strategies, such as adapter-based tuning and prompt-based tuning.

Discussion. Redundancy has two sides. One of the reason why VL-PMs can significantly improve the performance of the downstream tasks is that VL-PMs have learned rich and redundant knowledge in the pretraining process. Practically, for downstream tasks, especially in-domain tasks, task-related redundancy can help VL-PMs quickly adapt to the downstream tasks, while task-agnostic redundancy will simultaneously impair the robustness of systems. This paper investigates improving the robustness of systems while preserving their accuracy by seeking a tradeoff between representation compression and redundancy. Another potential study direction is to explore how to explicitly reduce task-agnostic redundancy and adequately exploit task-related redundancy when finetuning VL-PMs for the downstream tasks.

References

- [1] Stanislaw Antol, Aishwarya Agrawal, Jiasen Lu, Margaret Mitchell, Dhruv Batra, C Lawrence Zitnick, and Devi Parikh, “Vqa: Visual question answering,” in *CVPR*, 2015, pp. 2425–2433. 1
- [2] Zirui Wang, Jiahui Yu, Adams Wei Yu, Zihang Dai, Yulia Tsvetkov, and Yuan Cao, “Simvlm: Simple visual language model pretraining with weak supervision,” *arXiv preprint arXiv:2108.10904*, 2021. 1
- [3] Wenhui Wang, Hangbo Bao, Li Dong, and Furu Wei, “Vlmo: Unified vision-language pre-training with mixture-of-modality-experts,” *arXiv preprint arXiv:2111.02358*, 2021.
- [4] Junnan Li, Dongxu Li, Caiming Xiong, and Steven Hoi, “Blip: Bootstrapping language-image pre-training for unified vision-language understanding and generation,” *arXiv preprint arXiv:2201.12086*, 2022. 1
- [5] Vedika Agarwal, Rakshith Shetty, and Mario Fritz, “Towards causal vqa: Revealing and reducing spurious correlations by invariant and covariant semantic editing,” in *CVPR*, 2020, pp. 9690–9698. 1, 5, 9, 14, 15
- [6] Meet Shah, Xinlei Chen, Marcus Rohrbach, and Devi Parikh, “Cycle-consistency for robust visual question answering,” in *CVPR*, 2019, pp. 6649–6658. 1, 5, 6, 7, 9, 14, 15
- [7] Spencer Whitehead, Hui Wu, Yi Ren Fung, Heng Ji, Rogerio Feris, and Kate Saenko, “Learning from lexical perturbations for consistent visual question answering,” *arXiv preprint arXiv:2011.13406*, 2020. 1, 5, 9, 14, 15
- [8] Linjie Li, Jie Lei, Zhe Gan, and Jingjing Liu, “Adversarial vqa: A new benchmark for evaluating the robustness of vqa models,” *arXiv preprint arXiv:2106.00245*, 2021. 1, 6, 7, 9, 16
- [9] Sasha Sheng, Amanpreet Singh, Vedanuj Goswami, Jose Alberto Lopez Magana, Wojciech Galuba, Devi Parikh, and Douwe Kiela, “Human-adversarial visual question answering,” *arXiv preprint arXiv:2106.02280*, 2021. 1, 6, 9, 16
- [10] Naftali Tishby, Fernando C Pereira, and William Bialek, “The information bottleneck method,” *arXiv preprint physics/0004057*, 2000. 2, 9
- [11] Naftali Tishby and Noga Zaslavsky, “Deep learning and the information bottleneck principle,” in *ITW*, 2015, pp. 1–5. 2, 9
- [12] David Barber and Felix Agakov, “The im algorithm: a variational approach to information maximization,” in *NeurIPS*, 2003, pp. 201–208. 3
- [13] Mohamed Bennasar, Yulia Hicks, and Rossitza Setchi, “Feature selection using joint mutual information maximisation,” *Expert Systems with Applications*, vol. 42, no. 22, pp. 8520–8532, 2015. 3
- [14] Marco Federici, Anjan Dutta, Patrick Forré, Nate Kushman, and Zeynep Akata, “Learning robust representations via multi-view information bottleneck,” in *ICLR*, 2020. 3, 9, 20
- [15] Boxin Wang, Shuohang Wang, Yu Cheng, Zhe Gan, Ruoxi Jia, Bo Li, and Jingjing Liu, “InfoBERT: Improving robustness of language models from an information theoretic perspective,” in *ICLR*, 2021. 3, 9
- [16] Liunian Harold Li, Mark Yatskar, Da Yin, Cho-Jui Hsieh, and Kai-Wei Chang, “Visualbert: A simple and performant baseline for vision and language,” *arXiv preprint arXiv:1908.03557*, 2019. 4, 5, 6, 14, 16
- [17] Weijie Su, Xizhou Zhu, Yue Cao, Bin Li, Lewei Lu, Furu Wei, and Jifeng Dai, “VL-BERT: pre-training of generic visual-linguistic representations,” in *ICLR*, 2020. 5, 6, 9, 14
- [18] Yen-Chun Chen, Linjie Li, Licheng Yu, Ahmed El Kholy, Faisal Ahmed, Zhe Gan, Yu Cheng, and Jingjing Liu, “UNITER: Universal image-text representation learning,” in *ECCV*, 2020, pp. 104–120. 4, 5, 6, 7, 9, 14, 15, 16
- [19] Hao Tan and Mohit Bansal, “LXMERT: Learning cross-modality encoder representations from transformers,” in *EMNLP*, 2019, pp. 5099–5110. 4, 5, 6, 7, 9, 14, 16
- [20] Jiasen Lu, Dhruv Batra, Devi Parikh, and Stefan Lee, “ViLBERT: pretraining task-agnostic visiolinguistic representations for vision-and-language tasks,” in *NeurIPS*, 2019, pp. 13–23. 4, 5, 6, 9, 14, 16
- [21] Pengyu Cheng, Weituo Hao, Shuyang Dai, Jiachang Liu, Zhe Gan, and Lawrence Carin, “CLUB: A contrastive log-ratio upper bound of mutual information,” in *ICML*, 2020, pp. 1779–1788. 4, 7
- [22] Ben Poole, Sherjil Ozair, Aaron Van Den Oord, Alex Alemi, and George Tucker, “On variational bounds of mutual information,” in *ICML*, 2019, pp. 5171–5180. 5, 7

[23] Peter Anderson, Xiaodong He, Chris Buehler, Damien Teney, Mark Johnson, Stephen Gould, and Lei Zhang, “Bottom-up and top-down attention for image captioning and visual question answering,” in *CVPR*, 2018, pp. 6077–6086. [5](#), [15](#), [16](#)

[24] Ranjay Krishna, Yuke Zhu, Oliver Groth, Justin Johnson, Kenji Hata, Joshua Kravitz, Stephanie Chen, Yannis Kalantidis, Li-Jia Li, David A Shamma, et al., “Visual Genome: Connecting language and vision using crowdsourced dense image annotations,” *IJCV*, vol. 123, no. 1, pp. 32–73, 2017. [5](#), [14](#)

[25] Corentin Dancette, Remi Cadene, Damien Teney, and Matthieu Cord, “Beyond question-based biases: Assessing multimodal shortcut learning in visual question answering,” *arXiv preprint arXiv:2104.03149*, 2021. [5](#), [14](#), [16](#)

[26] Xinlei Chen, Hao Fang, Tsung-Yi Lin, Ramakrishna Vedantam, Saurabh Gupta, Piotr Dollár, and C Lawrence Zitnick, “Microsoft coco captions: Data collection and evaluation server,” *arXiv preprint arXiv:1504.00325*, 2015. [6](#), [14](#)

[27] XuanLong Nguyen, Martin J Wainwright, and Michael I Jordan, “Estimating divergence functionals and the likelihood ratio by convex risk minimization,” *IEEE Trans. Inf. Theory*, vol. 56, no. 11, pp. 5847–5861, 2010. [7](#)

[28] Aaron van den Oord, Yazhe Li, and Oriol Vinyals, “Representation learning with contrastive predictive coding,” *arXiv preprint arXiv:1807.03748*, 2018. [7](#)

[29] Mohamed Ishmael Belghazi, Aristide Baratin, Sai Rajeswar, Sherjil Ozair, Yoshua Bengio, Aaron Courville, and R Devon Hjelm, “mutual information neural estimation,” in *ICML*, 2018, pp. 530–539. [7](#)

[30] Yash Kant, Abhinav Moudgil, Dhruv Batra, Devi Parikh, and Harsh Agrawal, “Contrast and classify: Alternate training for robust vqa,” *arXiv preprint arXiv:2010.06087*, 2020. [9](#), [15](#)

[31] Yash Goyal, Tejas Khot, Douglas Summers-Stay, Dhruv Batra, and Devi Parikh, “Making the v in vqa matter: Elevating the role of image understanding in visual question answering,” in *CVPR*, 2017, pp. 6904–6913. [9](#), [14](#)

[32] Christopher Clark, Mark Yatskar, and Luke Zettlemoyer, “Don’t take the easy way out: Ensemble based methods for avoiding known dataset biases,” in *EMNLP*, 2019, pp. 4067–4080. [16](#)

[33] Damien Teney, Kushal Kafle, Robik Shrestha, Ehsan Abbasnejad, Christopher Kanan, and Anton van den Hengel, “On the value of out-of-distribution testing: An example of goodhart’s law,” in *NeurIPS*, 2020. [16](#)

[34] Corentin Kervadec, Grigory Antipov, Moez Baccouche, and Christian Wolf, “Roses are red, violets are blue... but should vqa expect them to?,” in *CVPR*, 2021, pp. 2776–2785.

[35] Jingjing Jiang, Ziyi Liu, Yifan Liu, Zhixiong Nan, and Nanning Zheng, “X-ggm: Graph generative modeling for out-of-distribution generalization in visual question answering,” in *ACM MM*, 2021, pp. 199–208. [9](#)

[36] Linjie Li, Zhe Gan, and Jingjing Liu, “A closer look at the robustness of vision-and-language pre-trained models,” *arXiv preprint arXiv:2012.08673*, 2020. [9](#), [15](#), [16](#)

[37] Ravid Shwartz-Ziv and Naftali Tishby, “Opening the black box of deep neural networks via information,” *arXiv preprint arXiv:1703.00810*, 2017. [9](#)

[38] Yingjun Du, Jun Xu, Huan Xiong, Qiang Qiu, Xiantong Zhen, Cees GM Snoek, and Ling Shao, “Learning to learn with variational information bottleneck for domain generalization,” in *ECCV*, 2020, pp. 200–216. [9](#)

[39] Bo Li, Yifei Shen, Yezhen Wang, Wenzhen Zhu, Colorado J Reed, Jun Zhang, Dongsheng Li, Kurt Keutzer, and Han Zhao, “Invariant information bottleneck for domain generalization,” *arXiv preprint arXiv:2106.06333*, 2021. [9](#)

[40] Kartik Ahuja, Ethan Caballero, Dinghuai Zhang, Yoshua Bengio, Ioannis Mitliagkas, and Irina Rish, “Invariance principle meets information bottleneck for out-of-distribution generalization,” *arXiv preprint arXiv:2106.06607*, 2021. [9](#)

[41] Feng Bao, “Disentangled variational information bottleneck for multiview representation learning,” *arXiv preprint arXiv:2105.07599*, 2021. [9](#)

[42] Rabeeh Karimi Mahabadi, Yonatan Belinkov, and James Henderson, “Variational information bottleneck for effective low-resource fine-tuning,” in *ICLR*, 2021. [9](#)

[43] Yann Dubois, Douwe Kiela, David J Schwab, and Ramakrishna Vedantam, “Learning optimal representations with the decodable information bottleneck,” in *NeurIPS*, 2020. 9

[44] Ziqi Pan, Li Niu, Jianfu Zhang, and Liqing Zhang, “Disentangled information bottleneck,” in *AAAI*, 2021, pp. 9285–9293. 9

[45] Insu Jeon, Wonkwang Lee, Myeongjang Pyeon, and Gunhee Kim, “Ib-gan: Disengangled representation learning with information bottleneck generative adversarial networks,” in *AAAI*, 2021, pp. 7926–7934. 9

[46] Zhicheng Huang, Zhaoyang Zeng, Bei Liu, Dongmei Fu, and Jianlong Fu, “Pixel-BERT: Aligning image pixels with text by deep multi-modal transformers,” *arXiv preprint arXiv:2004.00849*, 2020. 9

[47] Luowei Zhou, Hamid Palangi, Lei Zhang, Houdong Hu, Jason Corso, and Jianfeng Gao, “Unified vision-language pre-training for image captioning and vqa,” in *AAAI*, 2020, pp. 13041–13049.

[48] Lei Shi, Kai Shuang, Shijie Geng, Peng Su, Zhengkai Jiang, Peng Gao, Zuohui Fu, Gerard de Melo, and Sen Su, “Contrastive visual-linguistic pretraining,” *arXiv preprint arXiv:2007.13135*, 2020.

[49] Chenliang Li, Ming Yan, Haiyang Xu, Fuli Luo, Wei Wang, Bin Bi, and Songfang Huang, “SemVLP: Vision-language pre-training by aligning semantics at multiple levels,” *arXiv preprint arXiv:2103.07829*, 2021.

[50] Wonjae Kim, Bokyung Son, and Ildoo Kim, “Vilt: Vision-and-language transformer without convolution or region supervision,” in *ICML*, 2021, pp. 5583–5594. 9, 16

[51] Siqi Sun, Yen-Chun Chen, Linjie Li, Shuhang Wang, Yuwei Fang, and Jingjing Liu, “Lightningdot: Pre-training visual-semantic embeddings for real-time image-text retrieval,” in *ACL*, 2021, pp. 982–997.

[52] Zhicheng Huang, Zhaoyang Zeng, Yupan Huang, Bei Liu, Dongmei Fu, and Jianlong Fu, “Seeing out of the box: End-to-end pre-training for vision-language representation learning,” in *CVPR*, 2021, pp. 12976–12985. 9

[53] Zhe Gan, Yen-Chun Chen, Linjie Li, Chen Zhu, Yu Cheng, and Jingjing Liu, “Large-scale adversarial training for vision-and-language representation learning,” in *NeurIPS*, 2020. 9, 16

[54] Xiuju Li, Xi Yin, Chunyuan Li, Pengchuan Zhang, Xiaowei Hu, Lei Zhang, Lijuan Wang, Houdong Hu, Li Dong, Furu Wei, et al., “Oscar: Object-semantics aligned pre-training for vision-language tasks,” in *ECCV*, 2020, pp. 121–137.

[55] Pengchuan Zhang, Xiuju Li, Xiaowei Hu, Jianwei Yang, Lei Zhang, Lijuan Wang, Yejin Choi, and Jianfeng Gao, “VinVL: Revisiting visual representations in vision-language models,” *arXiv preprint arXiv:2101.00529*, 2021. 9

[56] Jiasen Lu, Vedanuj Goswami, Marcus Rohrbach, Devi Parikh, and Stefan Lee, “12-in-1: Multi-task vision and language representation learning,” in *CVPR*, 2020, pp. 10437–10446. 9

[57] Fei Yu, Jiji Tang, Weichong Yin, Yu Sun, Hao Tian, Hua Wu, and Haifeng Wang, “ERNIE-ViL: Knowledge enhanced vision-language representations through scene graph,” *arXiv preprint arXiv:2006.16934*, 2020.

[58] Yehao Li, Yingwei Pan, Ting Yao, Jingwen Chen, and Tao Mei, “Scheduled sampling in vision-language pretraining with decoupled encoder-decoder network,” *arXiv preprint arXiv:2101.11562*, 2021. 9

[59] Ashish Vaswani, Noam Shazeer, Niki Parmar, Jakob Uszkoreit, Llion Jones, Aidan N Gomez, Łukasz Kaiser, and Illia Polosukhin, “Attention is all you need,” in *NeurIPS*, 2017, pp. 5998–6008. 9

[60] Drew A Hudson and Christopher D Manning, “Gqa: A new dataset for real-world visual reasoning and compositional question answering,” in *CVPR*, 2019, pp. 6700–6709. 14

[61] Yuke Zhu, Oliver Groth, Michael Bernstein, and Li Fei-Fei, “Visual7w: Grounded question answering in images,” in *CVPR*, 2016, pp. 4995–5004. 14

[62] Piyush Sharma, Nan Ding, Sebastian Goodman, and Radu Soricut, “Conceptual captions: A cleaned, hypernymed, image alt-text dataset for automatic image captioning,” in *ACL*, 2018, pp. 2556–2565. 14

[63] Vicente Ordonez, Girish Kulkarni, and Tamara Berg, “Im2text: Describing images using 1 million captioned photographs,” *NeurIPS*, vol. 24, pp. 1143–1151, 2011. 14

[64] Yu Jiang, Vivek Natarajan, Xinlei Chen, Marcus Rohrbach, Dhruv Batra, and Devi Parikh, “Pythia v0. 1: the winning entry to the vqa challenge 2018,” *arXiv preprint arXiv:1807.09956*, 2018. 15

[65] Jin-Hwa Kim, Jaehyun Jun, and Byoung-Tak Zhang, “Bilinear attention networks,” in *NeurIPS*, 2018, pp. 1564–1574. [15](#)

[66] Ronghang Hu, Jacob Andreas, Trevor Darrell, and Kate Saenko, “Explainable neural computation via stack neural module networks,” in *ECCV*, 2018, pp. 53–69. [15](#)

[67] Jiaxin Shi, Hanwang Zhang, and Juanzi Li, “Explainable and explicit visual reasoning over scene graphs,” in *CVPR*, 2019, pp. 8376–8384. [15](#)

[68] Jiasen Lu, Xiao Lin, Dhruv Batra, and Devi Parikh, “Deeper lstm and normalized cnn visual question answering model,” https://github.com/VT-vision-lab/VQA_LSTM_CNN, 2015. [15](#)

[69] Vahid Kazemi and Ali Elqursh, “Show, ask, attend, and answer: A strong baseline for visual question answering,” *arXiv preprint arXiv:1704.03162*, 2017. [15](#)

[70] Zichao Yang, Xiaodong He, Jianfeng Gao, Li Deng, and Alex Smola, “Stacked attention networks for image question answering,” in *CVPR*, 2016, pp. 21–29. [16](#)

[71] Hedi Ben-Younes, Remi Cadene, Nicolas Thome, and Matthieu Cord, “Block: Bilinear superdiagonal fusion for visual question answering and visual relationship detection,” in *AAAI*, 2019, pp. 8102–8109. [16](#)

[72] Remi Cadene, Corentin Dancette, Matthieu Cord, Devi Parikh, et al., “RUBi: Reducing unimodal biases for visual question answering,” in *NeurIPS*, 2019, pp. 841–852. [16](#)

[73] Itai Gat, Idan Schwartz, Alexander Schwing, and Tamir Hazan, “Removing bias in multi-modal classifiers: Regularization by maximizing functional entropies,” in *NeurIPS*, 2020. [16](#)

[74] Robik Shrestha, Kushal Kafle, and Christopher Kanan, “A negative case analysis of visual grounding methods for vqa,” in *ACL*, 2020, pp. 8172–8181. [16](#)

[75] Junhyun Nam, Hyuntak Cha, Sung-Soo Ahn, Jaeho Lee, and Jinwoo Shin, “Learning from failure: De-biasing classifier from biased classifier,” in *NeurIPS*, 2020. [16](#)

[76] Long Chen, Xin Yan, Jun Xiao, Hanwang Zhang, Shiliang Pu, and Yueting Zhuang, “Counterfactual samples synthesizing for robust visual question answering,” in *CVPR*, 2020, pp. 10800–10809. [16](#)

[77] Jie Lei, Linjie Li, Luwei Zhou, Zhe Gan, Tamara L. Berg, Mohit Bansal, and Jingjing Liu, “Less is more: Clipbert for video-and-language learning via sparse sampling,” in *CVPR*, 2021. [16](#)

[78] Duy-Kien Nguyen, Vedanuj Goswami, and Xinlei Chen, “Movie: Revisiting modulated convolutions for visual counting and beyond,” in *ICLR*, 2021. [16](#)

[79] Douwe Kiela, Suvrat Bhooshan, Hamed Firooz, Ethan Perez, and Davide Testuggine, “Supervised multimodal bitransformers for classifying images and text,” *arXiv preprint arXiv:1909.02950*, 2019. [16](#)

[80] Ronghang Hu and Amanpreet Singh, “Unit: Multimodal multitask learning with a unified transformer,” *arXiv preprint arXiv:2102.10772*, 2021. [16](#)

[81] Ronghang Hu, Amanpreet Singh, Trevor Darrell, and Marcus Rohrbach, “Iterative answer prediction with pointer-augmented multimodal transformers for textvqa,” in *CVPR*, 2020, pp. 9992–10002. [16](#)

Appendices

This Appendix provides additional experimental results and the proof of **Theorem 1**.

A Additional Experimental Results

A.1 Details on VL-PTMs.

Table 6: A summary of baseline VL-PTMs. \dagger denotes the length of RoI features in each image is not fixed. The results marked in orange are re-implementations using the officially released code.

	VL-PTMs	Transformer Architecture	Pretraining Datasets	Visual Feature	VQA v2	
					test-dev	test-std
ID	VisualBERT [16]	single-stream encoder	COCO	100(RoI-2048)	70.80 70.46	71.00 -
ID + OOD	UNITER _B [18]	single-stream encoder	COCO, VG, CC, SUB	\dagger (RoI-2048+Loc-7)	72.70 71.63	72.91 -
	LXMERT [19]	two-stream encoders	COCO, VG, GQA, VQA v2, VG-QA	36(RoI-2048+Loc-4)	72.42 72.58	72.54 -
OOD	ViLBERT [20]	two-stream encoders	CC	\dagger (RoI-2048+Loc-5)	70.55 70.55	70.92 -
	VL-BERT _B [17]	single-stream encoder	CC	\dagger (RoI-2048+Loc-4)	71.16 71.20	- -

Table 6 summarizes the details of baseline VL-PTMs in our experiments. Specifically, we list the Transformer architecture of VL-PTMs, the pretraining datasets, the visual features (*i.e.*, image region features and location/position features), and the VQA-Score of the downstream VQA task on VQA v2. Pretraining datasets include MS COCO caption[26] (COCO), Visual Genome[24] (VG), VQA v2[31] (VQA v2), GQA balance version[60] (GQA), VG-QA[61] (VG-QA), Conceptual captions[62] (CC), and SBU captions[63] (SBU).

A.2 Evaluation on Input Robustness

A.2.1 Details on VQA Benchmarks of Input Robustness

Table 7: Benchmark details. len(Q) is the average question length. #IQ, #Pert, and #Ori denote the number of total image-question pairs, perturbation samples, and original samples.

Benchmark	Perturbation	Metric	QType	Train&Val		Test			
				#IQ	len(Q)	#IQ	len(Q)	#Pert/CE	#Ori/Easy
VQA-Rep[6]	Rephrasing	CS(k)	All	444K	6.20	162K	7.15	121,516	40,504
VQA P2[7]	Par&Syn&Ant	CS(k)	All	444K	6.20	52K	6.32	26,512	25,814
IV-VQA[5]	Invariant object	#flips	All	444K	6.20	120K	5.85	83,700	36,181
CV-VQA[5]	Covariant object	#flips	Num	444K	6.20	4K	5.83	4,141	2,641
VQA-CE[25]	Counterexample	-	All	444K	6.20	214K	6.19	63,298	147,681

Table 7 shows the details on VQA benchmark of input robustness, including perturbation type, robustness evaluation metric, question type, and statistics on train&val and test data. Specifically, **VQA-Rep** averagely collects 3 rephrasings for each of 40,504 questions sampled from the val set of VQA v2 [31], and obtains \sim 162K image-question pairs. **VQA P2** creates three types of linguistic perturbations, *i.e.*, Paraphrastic (Par), Synonymous (Syn), and Antonymous (Ant), for 25,814 sampled questions, finally obtains \sim 52K image-question pairs. **IV-VQA** is created using a GAN-based resynthesis technique to remove objects irrelevant to the QA pairs from the image (*i.e.*, removal of objects does not lead to any change in answer). Conversely, **CV-VQA** targets counting questions (Num) and removes one relevant object that makes the model prediction on the quantity of such objects are expected to be subtracted by 1. Finally, IV-VQA and CV-VQA have about 120K and 4K image-question pairs, respectively. **VQA-CE** is an evaluation protocol for multimodal shortcuts involved in images and questions. It leverages the detected shortcuts on training set to obtain 63,298 Counterexamples (*i.e.*, where all shortcuts provide an incorrect answer) from VQA v2 val set. Besides, it builds 147,681 easy examples on which at least one shortcut provides the correct answer.

Table 9: Comparisons with state-of-the-arts on VQA P2. Results in (I) are cited from the work [7].

#	Methods	Synonymous			Paraphrastic			Antonymous			All		
		Pert	Ori	CS(2)									
(I)	BAN[65]	64.50	66.30	-	56.30	56.70	-	73.90	86.00	-	-	-	-
	StackNMN[66]	61.20	63.50	64.70	53.20	53.60	53.80	74.80	84.90	76.10	63.30	66.90	66.20
	+ Q3R[7]	-	-	56.90	-	-	84.70	-	-	70.30	66.90	67.40	72.20
	HybridNet[7]	-	-	65.00	-	-	55.70	-	-	76.40	63.30	67.00	66.60
	+ Q3R[7]	-	-	70.80	-	-	59.40	-	-	83.70	67.00	67.40	72.50
	XNM[67]	62.80	65.20	67.60	55.60	56.80	60.70	74.30	85.10	76.00	64.70	68.30	68.80
(II)	+ Q3R[7]	-	-	72.90	-	-	61.80	-	-	84.70	68.10	68.90	74.40
	VisualBERT + CIB	68.62	70.98	73.31	59.44	60.40	63.45	78.28	88.04	81.01	69.92	73.15	73.83
	UNITER _B + CIB	70.03	72.32	75.36	61.84	62.16	66.86	79.25	89.57	82.93	71.30	74.52	75.91
	LXMERT + CIB	78.98	81.66	85.51	73.23	76.17	80.39	80.21	94.17	85.72	78.93	83.38	85.07
	ViLBERT + CIB	68.35	70.99	73.11	60.31	61.70	65.32	79.25	88.64	82.48	69.92	73.30	73.98
	VL-BERT + CIB	68.21	70.52	72.97	60.37	61.63	64.34	79.17	89.08	82.59	69.82	73.04	73.88

A.2.2 Comparisons with State-of-the-Arts

Comparisons on VQA-Rep.

Rep. Table 8 shows the complete comparisons with existing methods on VQA-Rep in terms of the VQA-Scores as well as CS(k). The results in (I) are cited from the work [6]. The result of (II) ① is cited from the work [36]. Considering the five baseline VL-PTMs (*i.e.*, VisualBERT, UNITER_B, LXMERT, ViLBERT, and VL-BERT), we evaluate the robustness of CIB against the linguistic variations, *i.e.*, the question rephrasings.

Overall, finetuning LXMERT and UNITER_B with our CIB respectively achieve the best and second best performance on the metrics of VQA-Score and CS(k). This results show that compared with existing methods, CIB is effective in finetuning VL-PTMs for VQA to improve the input robustness of the VQA model with respect to input linguistic variations. Since the VL-PTM, LXMERT, is pretrained on the VQA task, the best performance is far better than the second best performance.

Comparisons on VQA P2. Table 9 shows the results on VQA P2. Using VisualBERT, UNITER_B, LXMERT, ViLBERT, and VL-BERT as baseline VL-PTMs, we evaluate the robustness of the proposed CIB against the linguistic perturbation of Synonymous, Paraphrastic, and Antonymous. From the comparisons in the table, we can observe the advantage of CIB in improving the input robustness, especially the robustness against synonymous and paraphrastic perturbations.

Comparisons on IV-VQA and CV-VQA.

and CV-VQA. Table 10 show the comparisons with exiting methods on IV-VQA and CV-VQA. Using VisualBERT, UNITER_B, LXMERT, ViLBERT, and VL-BERT as baseline VL-PTMs, we also evaluate the robustness of our method against visual variations on the test splits of IV-VQA and CV-VQA. Results in (I) ① - ③ and results in (I) ④ are cited from the work [5]

Table 8: Comparisons with state-of-the-art methods on VQA-Rep.

#	Methods	VQA-Score		Robustness Metric			
		Pert	Ori	CS(1)	CS(2)	CS(3)	CS(4)
(I)	BUTD[23]	51.22	61.51	60.55	46.96	40.54	34.47
	+ CC[6]	52.58	62.44	61.66	50.79	44.68	42.55
	Pythia[64]	54.20	64.08	63.43	52.03	45.94	39.49
	+ CC[6]	55.65	64.52	64.36	55.45	50.92	44.30
	BAN[65]	55.87	64.97	64.88	53.08	47.45	39.87
	+ CC[6]	56.59	65.87	65.77	56.94	51.76	48.18
(II)	ConCAT[30]	-	-	68.62	61.42	57.08	53.99
	UNITER _B [18] ①	-	-	71.29	63.95	59.48	56.31
	MANGO[36]	-	-	72.66	66.03	61.92	58.95
(III)	VisualBERT + CIB	63.10	69.78	71.85	64.16	59.54	56.31
	UNITER _B + CIB	64.45	70.91	73.18	66.21	61.88	58.75
	LXMERT + CIB	72.62	80.93	82.01	75.46	71.05	67.71
	ViLBERT + CIB	62.28	69.15	71.05	63.54	59.04	55.89
	VL-BERT + CIB	60.86	68.74	70.52	63.46	58.75	53.89

Table 10: Comparisons on IV-VQA and CV-VQA.

#	Methods	IV-VQA			CV-VQA		
		Pert	Ori	#flips↓	Pert	Ori	#flips↓
(I)	CL[68]①	-	60.21	17.89	-	39.38	81.41
	SNMN[66]②	-	66.04	6.52	-	47.95	78.92
	SAAA[69]③	-	70.26	7.85	-	49.90	78.44
	UNITER _B [18]④	-	-	8.47	-	-	40.67
	MANGO[36]	-	-	7.32	-	-	38.11
(II)	VisualBERT + CIB	47.81	83.48	57.84	32.46	77.09	72.13
	UNITER _B + CIB	76.63	85.05	27.59	46.92	79.89	60.35
	LXMERT + CIB	78.57	94.15	23.10	40.47	93.90	61.39
	ViLBERT + CIB	74.67	83.35	30.04	35.33	71.11	73.53
	VL-BERT + CIB	73.66	83.37	30.41	35.29	72.70	74.18

and the work [36], respectively. The #flips is the ratio of the number of predictions mismatched before and after visual content manipulation to the total number of evaluation samples. Observed the results in Table 10, we find that compared with existing methods, CIB can better improve the ability of VQA models to defend against input visual variations.

Comparisons on VQA-CE. The comparisons with state-of-the-art methods on VQA-CE are summarized in Table 11. All results in group (I) and (II) are cited from the work [25]. Using VisualBERT, UNITER_B, LXMERT, ViLBERT, and VL-BERT as baseline VL-PTMs, we evaluate the robustness of our CIB against shortcut learning on VQA-CE. From the results in the table, we observe that the performance of finetuning baseline VL-PTMs with our CIB for VQA can surpass existing methods by a large margin, especially the VQA-Score on Counterexamples. This results suggest that the proposed CIB can better alleviate the spurious correlations between representations and the shortcut learning involved in inputs.

Table 11: Comparisons with state-of-the-arts on VQA-CE.

#	Methods	VQA-Score		
		CE	Easy	Overall
(I)	Shortcuts[25]	0.00	61.13	42.26
	SAN[70]	26.64	68.45	55.61
	BLOCK[71]	32.91	77.65	63.89
	BUTD[23]	33.91	76.69	63.52
	+ RUBi[72]	32.25	75.03	61.88
	+ LMH + RMFE[73]	33.14	73.32	60.96
	+ ESR[74]	33.26	76.18	62.96
	+ LMH[32]	34.26	73.12	61.15
	+ LfF[75]	34.27	76.60	63.57
	+ LMH + CSS[76]	34.36	62.08	53.55
(II)	+ RandImg[33]	34.41	76.21	63.34
	VilBERT[20]	39.24	80.50	67.77
	VisualBERT + CIB	40.86	81.25	68.80
	UNITER _B + CIB	42.03	82.48	70.00
	LXMERT + CIB	57.14	89.21	79.32
(III)	VilBERT + CIB	39.51	81.22	68.35
	VL-BERT + CIB	38.24	82.00	67.92

A.3 Evaluation on Human-Adversarial Robustness

Table 12: Comparisons on AVQA.

#	Methods	VQA-Score	
		test	val
(I)	<i>Training on VQA v2+VG-QA+AVQA.</i>		
	BUTD [23]	22.78	23.91
	ClipBERT [77]	24.35	24.24
	VILLA _B [53]	26.08	27.08
	VILLA _L [53]	25.32	26.32
	LXMERT [19]	24.13	25.24
	UNITER _B [18]	24.10	25.04
	UNITER _L [18]	24.78	26.27
(II)	<i>Training on AVQA train split.</i>		
	VisualBERT + CIB	24.55	24.78
	UNITER _B + CIB	25.71	25.89
	LXMERT + CIB	26.18	26.15
	VilBERT + CIB	26.55	26.49
	VL-BERT + CIB	26.35	26.38

Table 13: Comparisons on AdVQA.

#	Methods	VQA-Score	
		test	val
(I)	<i>Training on VQA v2 train+val split*.</i>		
	MoViE+MCAN [78]	26.64	26.37
	MMBT [79]	26.70	25.78
	UniT [80]	28.15	27.55
	VisualBERT [16]	28.70	28.03
	VilBERT [20]	27.36	27.36
	ViLT [50]	27.11	27.19
	UNITER-B [18]	25.16	25.20
	VILLA-B [53]	25.14	25.17
	UNITER-L [18]	26.94	28.03
(II)	<i>Training on AVQA train split.</i>		
	VisualBERT + CIB	38.20	38.45
	UNITER _B + CIB	37.55	38.00
	LXMERT + CIB	37.24	38.91
	VilBERT + CIB	37.63	38.05
	VL-BERT + CIB	37.43	39.39

Comparisons on AVQA and AdVQA. Table 12 and Table 13 summarize the comparisons with state-of-the-art methods on AVQA and AdVQA, respectively. Using VisualBERT, UNITER_B, LXMERT, VilBERT, and VL-BERT as baseline VL-PTMs, we finetune them with CIB for VQA and evaluate the human-adversarial robustness of VQA systems. Results in Table 12 (I) and results in Table 13 are cited from the work [8] and the work [9], respectively. In addition to the train split of AVQA, the compared methods in Table 12 (I) and Table 13 (I) also utilize additional datasets when finetuning for VQA. However, compared with existing methods, our methods achieve the best performance only using the AVQA dataset.

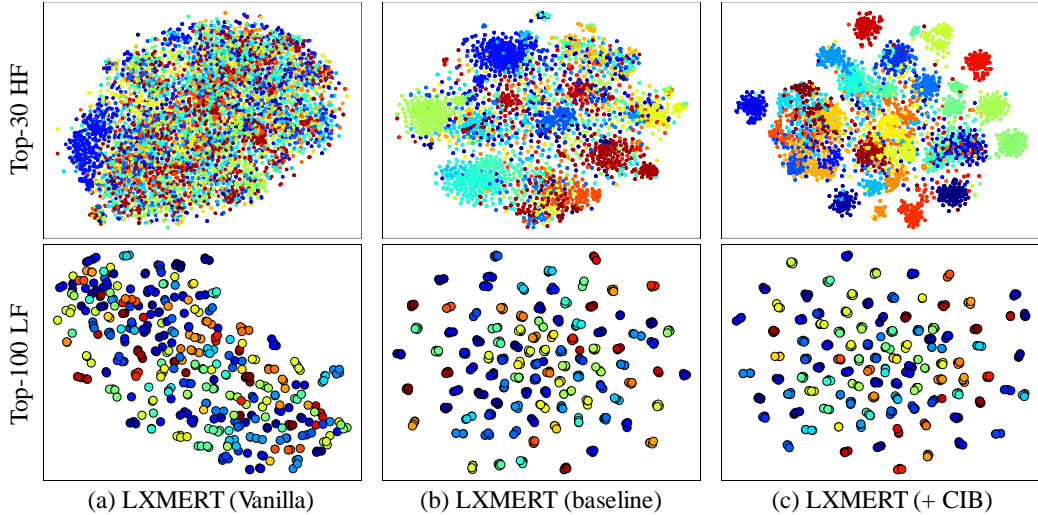


Figure 4: t-SNE visualization of the representations with regard to top-30 high-frequency and top-100 low-frequency answers on VQA-Rep.

A.4 Visualization

Figure 4 shows the t-SNE plot of the representation Z obtained by LXMERT for answer prediction on VQA-Rep. To better visualize the differences, we only consider the representations with regard to the top-30 high-frequency and top-100 low-frequency answers. Compared to the vanilla implementation (LXMERT without pretrained weights) and the baseline (pretrained LXMERT without CIB), finetuning LXMERT with CIB can advance the discriminability of the obtained representation.

B Proofs

B.1 Proof of Theorem 1

To prove **Theorem 1** in the main text, we first enumerate some of the properties of mutual information (MI) and then state two easily proven Lemmas.

B.1.1 Statements

Properties of MI. For any random variables X , Y and Z :

(P_1) Positivity:

$$I(X; Y) \geq 0, I(X; Y|Z) \geq 0.$$

(P_2) Chain rule:

$$\begin{aligned} I(X, Y; Z) &= I(Y; Z) + I(X; Z|Y) \\ &= I(X; Z) + I(Y; Z|X) \\ &= \frac{1}{2}[I(Y; Z) + I(X; Z) + I(X; Z|Y) + I(Y; Z|X)]. \end{aligned}$$

(P_3) Chain rule (Multivariate Mutual Information):

$$I(X; Y; Z) = I(Y; Z) - I(Y; Z|X).$$

(P_4) Positivity of discrete entropy (for discrete X):

$$H(X) \geq 0, H(X|Y) \geq 0.$$

(P_5) Entropy and Mutual Information:

$$H(X) = H(X|Y) + I(X; Y).$$

Lemma B.1. In representation learning, given a random variable X , the random variable Z is defined to be a representation of X , we can simply state that Z is conditionally independent from any other variable in the model once X is observed. That is, for any variable (or groups of variables) T_1 and T_2 in the model, we have

$$I(Z; T_1 | X, T_2) = 0.$$

Lemma B.2. Given a sequence of random variables X_1, X_2, \dots, X_n and a deterministic function f , then $\forall i, j = 1, 2, \dots, n$, we have

$$I(X_i; f(X_i)) \geq I(X_j; f(X_i)).$$

Proof. By the definition,

$$\begin{aligned} I(X_i; f(X_i)) &= H(f(X_i)) - H(f(X_i) | X_i), \\ I(X_j; f(X_i)) &= H(f(X_i)) - H(f(X_i) | X_j). \end{aligned}$$

Since f is a deterministic function,

$$\begin{aligned} H(f(X_i) | X_i) &= 0, \\ H(f(X_i) | X_j) &\geq 0. \end{aligned}$$

Therefore,

$$I(X_i; f(X_i)) \geq I(X_j; f(X_i)).$$

□

Lemma B.3. Let Z_1 and Z_2 are the representation of X_1 and X_2 , respectively, then

$$\begin{aligned} I_\theta(X_1; Z_1 | X_2) &\leq D_{\text{KL}}(p_\theta(Z_1 | X_1) || p_\psi(Z_2 | X_2)), \\ I_\psi(X_2; Z_2 | X_1) &\leq D_{\text{KL}}(p_\psi(Z_2 | X_2) || p_\theta(Z_1 | X_1)). \end{aligned}$$

Proof. By the definition,

$$\begin{aligned} I_\theta(X_1; Z_1 | X_2) &= \mathbb{E}_{x_1, x_2 \sim p(X_1, X_2)} \mathbb{E}_{z \sim p_\theta(Z_1 | X_1)} \left[\log \frac{p_\theta(Z_1 = z | X_1 = x_1)}{p_\theta(Z_1 = z | X_2 = x_2)} \right] \\ &= \mathbb{E}_{x_1, x_2 \sim p(X_1, X_2)} \mathbb{E}_{z \sim p_\theta(Z_1 | X_1)} \left[\log \frac{p_\theta(Z_1 = z | X_1 = x_1)}{p_\psi(Z_2 = z | X_2 = x_2)} \right] \\ &\quad - \mathbb{E}_{x_1, x_2 \sim p(X_1, X_2)} \mathbb{E}_{z \sim p_\theta(Z_1 | X_1)} \left[\log \frac{p_\theta(Z_1 = z | X_2 = x_2)}{p_\psi(Z_2 = z | X_2 = x_2)} \right] \\ &= D_{\text{KL}}(p_\theta(Z_1 | X_1) || p_\psi(Z_2 | X_2)) - D_{\text{KL}}(p_\theta(Z_2 | X_1) || p_\psi(Z_2 | X_2)) \\ &\leq D_{\text{KL}}(p_\theta(Z_1 | X_1) || p_\psi(Z_2 | X_2)). \end{aligned}$$

If and only if $p_\psi(Z_2 | X_2)$ coincides with $p_\theta(Z_1 | X_2)$, the equality holds. Analogously, we can derive $I_\psi(X_2; Z_2 | X_1) \leq D_{\text{KL}}(p_\psi(Z_2 | X_2) || p_\theta(Z_1 | X_1))$. □

B.1.2 Proof of Theorem 1

Theorem 1. (*Upper Bound of $I(X^v, X^l; T^v, T^l)$*) Given two groups of random variables $X = [X^v, X^l]$, $T = [T^v, T^l]$, the mutual information $I(X^v, X^l; T^v, T^l)$ can be upper-bounded with

$$I(X; T) = I(X^v, X^l; T^v, T^l) \leq \underbrace{I(X^v; T^v)}_{\textcircled{1}} + \underbrace{I(X^l; T^l)}_{\textcircled{2}} - \underbrace{I(T^v; T^l)}_{\textcircled{3}} + \underbrace{D_{\text{SKL}}}_{\textcircled{4}}, \quad (12)$$

where D_{SKL} denotes the Symmetric Kullback-Leibler divergence and can be obtained by averaging the two Kullback-Leibler divergence, $D_{\text{KL}}(p(t^v | x^v) || p(t^l | x^l))$ and $D_{\text{KL}}(p(t^l | x^l) || p(t^v | x^v))$.

Proof.

$$\begin{aligned} I(X; T) &= I(X^l, X^v; T) \stackrel{(P_2)}{=} \frac{1}{2}[I(X^l; T) + I(X^v; T) + I(X^l; T|X^v) + I(X^v; T|X^l)] \\ &= \frac{1}{2}[I(X^l; T^l, T^v) + I(X^v; T^l, T^v) + I(X^l; T|X^v) + I(X^v; T|X^l)] \end{aligned}$$

Since,

$$\begin{aligned} I(X^l; T^l, T^v) &\stackrel{(P_2)}{=} I(X^l; T^l) + I(X^l; T^v|T^l) \\ &\stackrel{(P_3)}{=} I(X^l; T^l) + I(X^l; T^v) - I(X^l; T^v; T^l) \\ &\stackrel{(P_3)}{=} I(X^l; T^l) + I(X^l; T^v) - I(T^l; T^v) + I(T^l; T^v|X^l) \\ &\stackrel{(LA.1.)}{=} I(X^l; T^l) + I(X^l; T^v) - I(T^l; T^v) \\ &\stackrel{(LA.2.)}{\leq} 2I(X^l; T^l) - I(T^l; T^v). \end{aligned}$$

Analogously, $I(X^v; T^l, T^v)$ is upper bounded by

$$I(X^v; T^l, T^v) \leq 2I(X^v; T^v) - I(T^l; T^v).$$

And,

$$\begin{aligned} I(X^l; T|X^v) &= I(X^l; T^l, T^v|X^v) \\ &\stackrel{(P_2)}{=} I(X^l; T^l|X^v) + I(X^l; T^v|X^v, T^l) \\ &\stackrel{(LA.1.)}{=} I(X^l; T^l|X^v), \\ I(X^v; T|X^l) &= I(X^v; T^l, T^v|X^l) \\ &\stackrel{(P_2)}{=} I(X^v; T^v|X^l) + I(X^v; T^l|X^l, T^v) \\ &\stackrel{(LA.1.)}{=} I(X^v; T^v|X^l). \end{aligned}$$

Let $D_{\text{SKL}} = \frac{1}{2}(D_{\text{KL}}(p_\theta||p_\psi) + D_{\text{KL}}(p_\psi||p_\theta))$,
therefore,

$$\begin{aligned} I(X; T) &= I(X^l, X^v; T^l, T^v) \\ &\leq I(X^l; T^l) + I(X^v; T^v) - I(T^l; T^v) + \frac{1}{2}[I(X^l; T^l|X^v) + I(X^v; T^v|X^l)] \\ &\stackrel{(LA.3.)}{\leq} I(X^l; T^l) + I(X^v; T^v) - I(T^l; T^v) \\ &\quad + \frac{1}{2}[D_{\text{KL}}(p_\theta(T_1|X_1)||p_\psi(T_2|X_2)) + D_{\text{KL}}(p_\psi(T_2|X_2)||p_\theta(T_1|X_1))] \\ &= I(X^l; T^l) + I(X^v; T^v) - I(T^l; T^v) + D_{\text{SKL}}. \end{aligned}$$

□

B.2 Proof of Alternatives in Section 3.4

In this section, we provide the derivations of the meaningful combinations of terms in Eq.(5), *i.e.*, the three alternatives in Section 3.4.

Proof of $I(X^l, X^v; T^l, T^v) \leq \frac{3}{2}[I(X^v; T^v) + I(X^l; T^l)]$.

Proof.

$$\begin{aligned}
I(X^l, X^v; T^l, T^v) &\leq I(X^l; T^l) + I(X^v; T^v) - I(T^l; T^v) + \frac{1}{2}[I(X^l; T^l|X^v) + I(X^v; T^v|X^l)] \\
&\leq I(X^l; T^l) + I(X^v; T^v) + \frac{1}{2}[I(X^l; T^l|X^v) + I(X^v; T^v|X^l)] \\
&\leq I(X^l; T^l) + I(X^v; T^v) + \frac{1}{2}[I(X^l; T^l) + I(X^v; T^v)] \\
&= \frac{3}{2}[I(X^l; T^l) + I(X^v; T^v)].
\end{aligned}$$

□

Proof of $I(X^l, X^v; T^l, T^v) \leq -I(T^v; T^l) + D_{\text{SKL}}$. Please see the work of Federici *et al.* [14].

Proof of $I(X^l, X^v; T^l, T^v) \leq I(X^v; T^v) + I(X^l; T^l) + D_{\text{SKL}}$.

Proof.

$$\begin{aligned}
I(X^l, X^v; T^l, T^v) &\stackrel{(\text{Theorem 1.})}{\leq} I(X^l; T^l) + I(X^v; T^v) - I(T^l; T^v) + D_{\text{SKL}} \\
&\stackrel{(I(T^l; T^v) \geq 0)}{\leq} I(X^l; T^l) + I(X^v; T^v) + D_{\text{SKL}}.
\end{aligned}$$

□